ASTROBIOLOGY
Volume 10, Number 4, 2010

DOI: 10.1089/ast.2009.0426

Diversity in the Archean Biosphere: New Insights from NanoSIMS

Dorothy Z. Oehler,[1] François Robert,[2] Malcolm R. Walter,[3] Kenichiro Sugitani,[4] Anders Meibom,[2] Smail Mostefaoui,[2] and Everett K. Gibson[1]

Abstract

The origin of organic microstructures in the ~3 Ga Farrel Quartzite is controversial due to their relatively poor state of preservation, the Archean age of the cherts in which they occur, and the unusual spindle-like morphology of some of the forms. To provide more insight into the significance of these microstructures, nano-scale secondary ion mass spectrometry (NanoSIMS) maps of carbon, nitrogen, sulfur, silicon, and oxygen were obtained for spheroidal and spindle-shaped constituents of the Farrel Quartzite assemblage. Results suggest that the structures are all bona fide ~3 Ga microfossils.

The spindles demonstrate an architecture that is remarkable for 3 Ga organisms. They are relatively large, robust, and morphologically complex. The NanoSIMS element maps corroborate their complexity by demonstrating an intricate, internal network of organic material that fills many of the spindles and extends continuously from the body of these structures into their spearlike appendages.

Results from this study combine with previous morphological and chemical analyses to argue that the microstructures in the Farrel Quartzite comprise a diverse assemblage of Archean microfossils. This conclusion adds to a growing body of geochemical, stromatolitic, and morphological evidence that indicates the Archean biosphere was varied and well established by at least ~3 Ga. Together, the data paint a picture of Archean evolution that is one of early development of morphological and chemical complexity. The evidence for Archean evolutionary innovation may augur well for the possibility that primitive life on other planets could adapt to adverse conditions by ready development of diversity in form and biochemistry. Key Words: NanoSIMS—Archean—Pilbara—Organic microfossil—Spindle—Microstructure—Early evolution—Farrel Quartzite. Astrobiology 10, 413–424.

1. Introduction

Archean life, especially that 3 Ga and older, is a concept that has drawn controversy (García-Ruiz *et al.*, 2002, 2003; Lindsay *et al.*, 2003; Moorbath, 2005; Brasier *et al.*, 2006). Doubt has been raised by discussions of (1) pseudofossils (biomorphs) that might explain putative Archean microfossils, (2) abiotic structures that could mimic microbially produced stromatolites, and (3) uncertainty as to syngeneity of complex biomarkers [*e.g.*, a study that identified Archean biomarkers suggestive of eukaryotes and cyanobacteria (Brocks *et al.*, 1999) has been reinterpreted in light of new data (Rasmussen *et al.*, 2008), with the conclusion that the biomarkers are not syngenetic but entered the rock sometime after the Archean].

At the same time, there is a growing body of data suggestive of Archean microbial diversity. These data include assessments of both organic microstructures and stromatolites (Walter *et al.*, 1980; Schopf, 1993, 2006; Hofmann *et al.*, 1999; Altermann and Kazmierczak, 2003; Allwood *et al.*, 2006, 2009; Schopf and Walter, 2007; Schopf *et al.*, 2007; Sugitani *et al.*, 2007; Rasmussen, 2000; Rasmussen *et al.*, 2009; Javaux *et al.*, 2010) as well as geochemical, electron microscopic, spectroscopic, and molecular studies that suggest biogenicity and syngeneity of Archean carbonaceous residues (Eigenbrode and Freeman, 2006; De Gregorio and Sharp, 2007; Duck *et al.*, 2007; Marshall *et al.*, 2007; Van Zuilen *et al.*, 2007; Derenne *et al.*, 2008; De Gregorio *et al.*, 2009; Oehler *et al.*, 2009; Waldbauer *et al.*, 2009).

[1]Astromaterials Research and Exploration Science, NASA, Johnson Space Center, Houston, Texas, USA.
[2]Laboratoire de Minéralogie et Cosmochimie du Muséum (LMCM), Muséum National d'Histoire Naturelle, Paris, France.
[3]Australian Centre for Astrobiology, University of New South Wales, Kensington, Australia.
[4]Department of Environmental Engineering and Architecture, Graduate School of Environmental Studies, Nagoya University, Nagoya, Japan.

A recently described assemblage of organic microstructures in cherts from the ~3 Ga Farrel Quartzite of Western Australia adds significantly to the list of potential Archean microbiota (Sugitani *et al.,* 2007, 2009a, 2009b). Laser Raman spectroscopy has shown that the microstructures are composed of disordered carbon, and $\delta^{13}C$ values $< -30‰$ of bulk carbon extracted from the Farrel Quartzite cherts suggest a biological origin for the carbonaceous constituents. While the studies of Sugitani *et al.* (2007, 2009a, 2009b) and Grey and Sugitani (2009) have suggested that many of the structures in the Farrel Quartzite are likely to be of biological derivation, their interpretations have been cautious, as the structures are relatively poorly preserved, occur in sediments of great age, and include unusual spindle-like forms. If biogenicity as well as syngeneity could be further substantiated, this material would represent one of the oldest known, relatively diverse microbiotas, and it would add substantially to our knowledge of the early biosphere.

Nano-scale secondary ion mass spectrometry (NanoSIMS) is one of many new techniques being applied to ancient organic materials in sedimentary rocks. The advantage of this technique is that the optimization for small beam size allows determination of elemental composition of individual microstructures, and results thus can be compared with optical or electron microscopic images of the same material. In addition, the technique can measure metabolically important elements of carbon, nitrogen, and sulfur; and, since organic material is analyzed in polished thin section, relationships to the surrounding mineral matrix and veins or fractures can be assessed as well.

Previous NanoSIMS analyses (Oehler *et al.,* 2006) of well-preserved Proterozoic microfossils from the ~0.83 Ga Bitter Springs Formation (Schopf, 1968; Schopf and Blacic, 1971) established submicron-scale distributions of carbon ($^{12}C^-$), nitrogen (measured as $^{12}C^{14}N^-$), and sulfur ($^{32}S^-$) that characterize undisputed microfossils. Results suggest that the strongest indicators of biogenicity are (1) a one-to-one correspondence of C^- and CN^- with kerogenous structures observed in optical microscopy, (2) globular, aligned concentrations of C^- and CN^-, and (3) parallel variations in C^- and CN^- concentrations. More recent NanoSIMS work suggests that associations between organic structures and enhanced concentrations of silicon ($^{28}Si^-$) and oxygen ($^{16}O^-$) are likely to reflect silica permineralization of microbial remains and thus can be indicators of syngeneity (Oehler *et al.,* 2009).

This study utilizes NanoSIMS to further address the biogenicity and syngeneity of the organic microstructures in the Archean Farrel Quartzite.

2. Materials and Methods

NanoSIMS elemental analyses were obtained on individual microstructures in 30 μm polished thin sections of chert from the Mt. Grant locality of the ~3 Ga Farrel Quartzite (Sugitani *et al.,* 2007). Individual microstructures were located within the thin sections via optical microscopy. Specimens at the top of the sections were selected for NanoSIMS and photographed with an Olympus BX60 Research, Polarizing Optical Microscope, outfitted with a Nikon DXM 1200F Digital Camera. Photomicrographs were taken in transmitted and reflected light, and sketch maps were constructed for use with the photographs for locating the specimens in the NanoSIMS. Photomicrographic focal series were taken from the top of the thin section to the base of the structures of interest in transmitted light by using a 100× oil immersion lens and Cargill type DF immersion oil (Formula Code 1261). The thin sections were subsequently cleaned by ultrasonication five times with reagent-grade ethanol for 2 minutes each time. The thin sections were dried in a 60°C oven for 1 hour to drive off the ethanol, and they were coated with about 300 Å of gold. It was assumed that the ultrasonication procedure was adequate to remove traces of immersion oil. This assumption is reasonable in view of the following:

(1) Initial sputtering by NanoSIMS removes surface contamination before data are collected, and none of the structures imaged resides in a crack in the thin section where traces of immersion oil conceivably could remain after sputtering.
(2) The NanoSIMS carbon maps are mirrored by nitrogen and sulfur maps and thus are suggestive of sedimentary organic matter rather than immersion oil (which is composed only of hydrocarbons and lacks nitrogen and sulfur).
(3) There is a one-to-one correspondence of the carbon, sulfur, and nitrogen maps with optical microscopic images of the kerogenous structures.

Chemical maps were produced with the Cameca NanoSIMS 50 at the National NanoSIMS facility at the Muséum National d'Histoire Naturelle in Paris, France. By using a focused primary beam of cesium (Cs^+; beam current ~1 pA, beam dwell time 1000 microseconds per pixel), secondary ions of carbon ($^{12}C^-$), nitrogen (measured as $^{12}C^{14}N^-$), sulfur ($^{32}S^-$), silicon ($^{28}Si^-$), and oxygen ($^{16}O^-$) were sputtered from the sample surface and detected simultaneously (multi-collection mode) in electron multipliers at a mass-resolving power of ~4,500 ($M/\Delta M$). At this mass-resolving power, the measured secondary ions were resolved from potential interference by other ions or molecules that fall close in mass to the ions of interest. Because nitrogen is measured as CN^-, it can only be detected in the presence of carbon.

Images were obtained from a presputtered area by stepping the primary beam across the sample surface. Presputtering was done to clean the surface of contaminants before analysis, remove the conductive coating, and implant Cs^+ ions in the material to be analyzed. The primary beam was focused to a spot size of ~50–100 nm, and the step size was adjusted so that it was slightly smaller than the primary beam. An electron gun (e-gun) supplied electrons to the sputtered surface during analysis to compensate for positive charge deposition from the primary beam and minimize specimen charging effects. Near steady state was reached where a reproducible, flat plateau was obtained in the secondary ion emission.

A charcoal sample was used as a standard. Kerogen was prepared from charcoal by HF-HCl maceration, and the elemental composition of the kerogen was measured by standard chemical techniques (Beaumont and Robert, 1999). The results from NanoSIMS analyses for each element were compared to those from the chemical analyses. The kerogen standard was included in the same mount with the Farrel Quartzite samples and was analyzed by NanoSIMS at the beginning and end of each session and between samples. Identical operating conditions in the NanoSIMS (*e.g.,* same

presputtering, spot size, e-gun) were used for analyzing the standard and the Precambrian structures. Elemental results from the Precambrian samples measured by NanoSIMS were normalized to results from the standard.

The NanoSIMS results were processed with L'Image software developed by L. Nittler, Carnegie Institution of Washington, Washington DC.

3. Results

NanoSIMS element maps were obtained for three categories of microstructures in cherts of the Farrel Quartzite: small spheroids, large spheroids, and spindle-shaped structures (Figs. 1–5). Comparisons were made with NanoSIMS element distributions in both undisputed microfossils from the ~0.83 Ga Bitter Springs Formation and secondary carbonaceous material in a hydrothermal vein in an Archean sample from the ~3.4 Ga Strelley Pool Chert (Oehler *et al.*, 2006, 2008a, 2008b, 2008c, 2009). For biogenicity assessment, characteristics utilized were the C^- and CN^- responses (size, shape, alignment and continuity), the relationship between intensities of C^- and CN^-, and the spatial relationships of C^- and CN^- to microstructures imaged in optical photomicrographs. For syngeneity assessment, Si^- and O^- concentrations

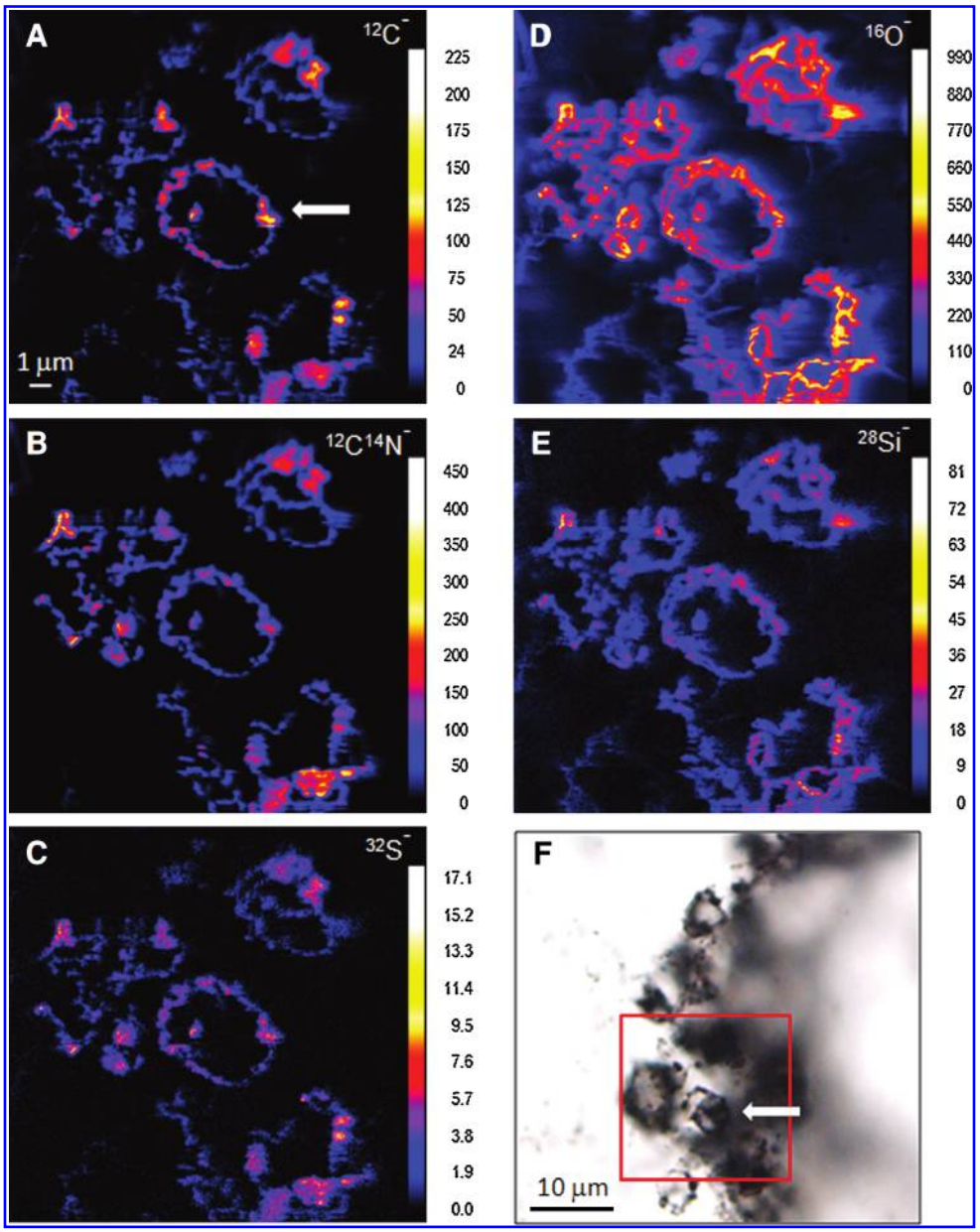

FIG. 1. NanoSIMS element maps of small spheroids in chert from the Farrel Quartzite of Western Australia. (**A–E**) NanoSIMS maps for carbon ($^{12}C^-$), nitrogen ($^{12}C^{14}N^-$), sulfur ($^{32}S^-$), oxygen ($^{16}O^-$), and silicon ($^{28}Si^-$). Color bars and scales indicate yield of ions (intensity of response). The scales are set by the image processing software. (**F**) Optical photomicrograph in transmitted light of a cluster of small spheroids, showing the area (red rectangle) imaged by NanoSIMS in (A–E). Arrows in (A) and (F) point to the same structure. Scale bar in (A) applies to (A–E).

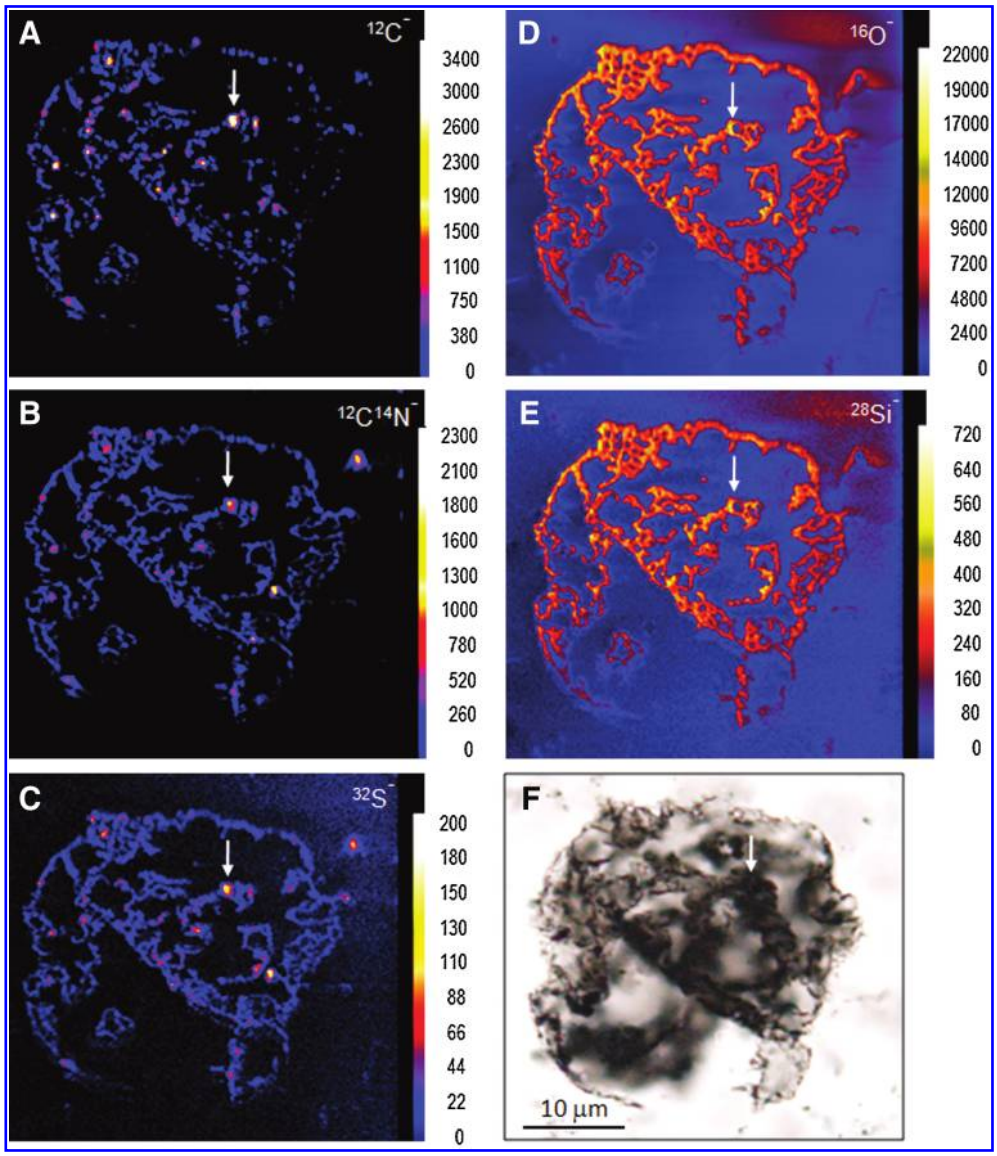

FIG. 2. NanoSIMS element maps of a large spheroid in chert from the Farrel Quartzite. (**A–E**) NanoSIMS maps for carbon ($^{12}C^-$), nitrogen ($^{12}C^{14}N^-$), sulfur ($^{32}S^-$), oxygen ($^{16}O^-$), and silicon ($^{28}Si^-$). Color bars and scales indicate yield of ions (intensity of response). The scales are set by the image processing software. (**F**) Optical photomicrograph in transmitted light of the large spheroid imaged by NanoSIMS in (A–E). Arrows in (A–F) illustrate one of the granules with high $^{12}C^-$, $^{12}C^{14}N^-$, and $^{32}S^-$. Scale bar in (F) applies to (A–F).

were compared to C^- and CN^- concentrations as well as to indications of Si^- and O^- in the chert matrix.

Results imply that the microstructures analyzed from the Farrel Quartzite are both biogenetic in derivation and syngenetic to the chert in which they are preserved.

3.1. Small spheroids

Small spheroids have been described from this assemblage based largely on optical microscopy (Sugitani *et al.*, 2007, 2009b). These spheroids (Fig. 1F) range in diameter from less than 5 μm to about 15 μm and occur in irregular clusters of a few to a few tens of individuals. The spheroids commonly appear to be loosely joined by strandlike connections or diffuse mucilaginous-like material. Within a cluster, individual cell-like bodies are irregularly and rather poorly preserved. No obvious internal contents have been noted. The walls of these spheroids are irregularly granular. More than 300 specimens in this category were documented by Sugitani *et al.* (2007).

NanoSIMS element maps of a cluster of small spheroids are shown in Fig. 1A–E. Figure 1F shows an optical photomicrograph of the cluster, and the red rectangle illustrates the portion of that cluster that was analyzed by NanoSIMS. Most of the spheroids in this grouping are between about 4 and 7 μm in diameter. Since NanoSIMS analysis investigates only the topmost several nanometers of thin sections, three-dimensional structures that can be observed in optical microscopy are frequently only partially imaged in NanoSIMS. Consequently, the NanoSIMS element maps of the cluster of small spheroids captured only fragments of five individual

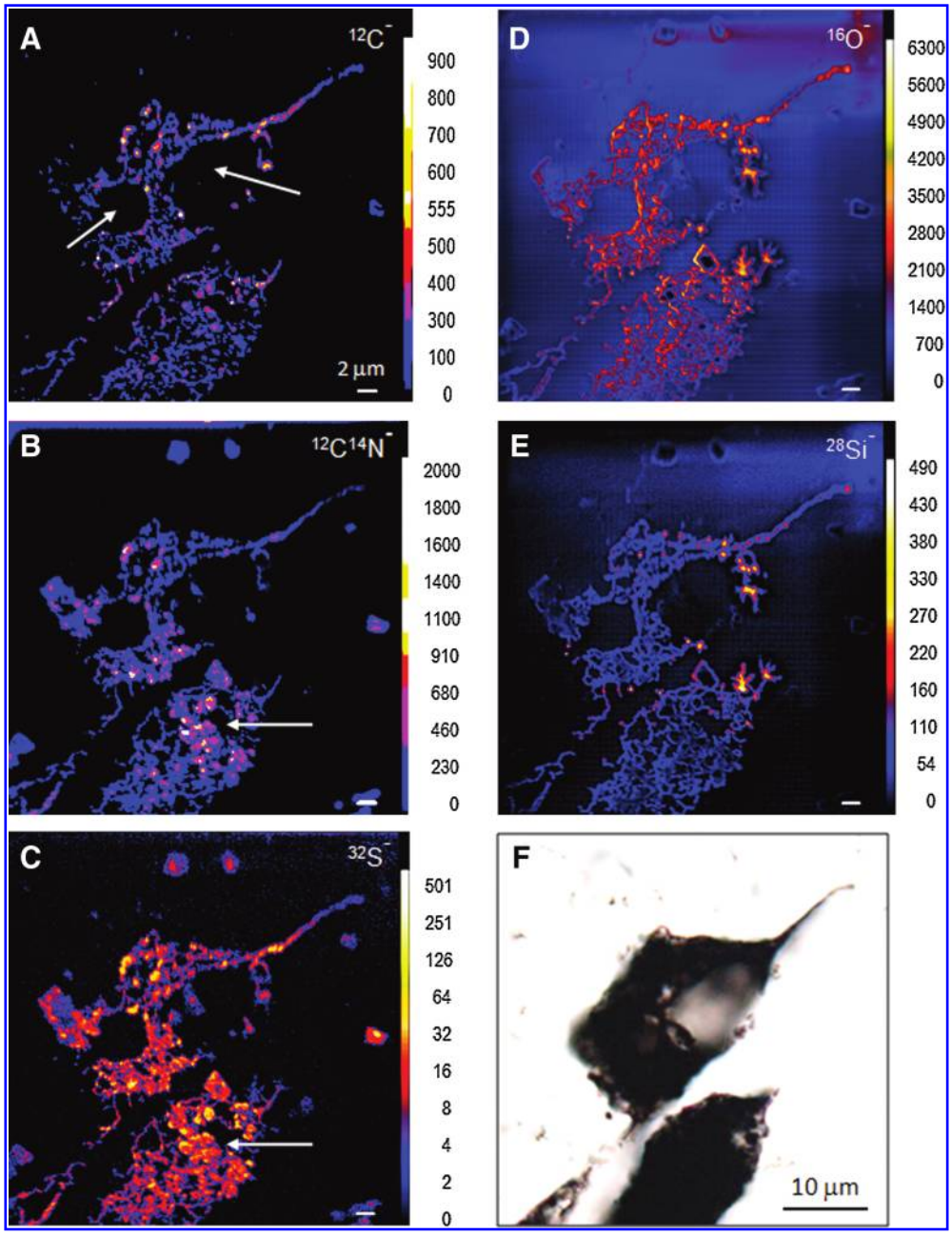

FIG. 3. NanoSIMS element maps of two spindles in chert from the Farrel Quartzite. (**A**–**E**) NanoSIMS maps for carbon ($^{12}C^-$), nitrogen ($^{12}C^{14}N^-$), sulfur ($^{32}S^-$), oxygen ($^{16}O^-$), and silicon ($^{28}Si^-$). Color bars and scales indicate yield of ions (intensity of response). The scales are set by the image processing software. (**F**) Optical photomicrograph in transmitted light of the spindles imaged by NanoSIMS in (A–E). Arrows in (A) point to cavities. Arrows in (B) and (C) point to patches having unusually high $^{12}C^{14}N^-$ and $^{32}S^-$ responses. Scale bar in (A) applies to (A–E).

structures. The structure at the center of this grouping was captured almost in its entirety, yielding secondary ions from the nearly complete perimeter. In the other four structures, the NanoSIMS maps yielded secondary ions from more irregular portions of the spheroids. Nevertheless, all the analyzed fragments of these small spheroids have the following characteristics in common:

- The distribution maps of C^-, CN^-, and S^- have a one-to-one correspondence with the structures observed by optical microscopy (Fig. 1A–C, F);
- Variations in C^-, CN^-, and S^- concentrations parallel one another (Fig. 1A–C);
- The C^-, CN^-, and S^- responses correspond to aligned element concentrations that are partially contiguous and form enveloping, wall-like boundaries (Fig. 1A–C).
- The C^-, CN^-, and S^- concentrations are globular and $\sim$0.2 to 0.5 μm thick, and they have generally rounded edges (Fig. 1A–C).
- Si^- and O^- maps demonstrate high concentrations of these elements immediately surrounding the carbonaceous material of the spheroids. The concentrations of

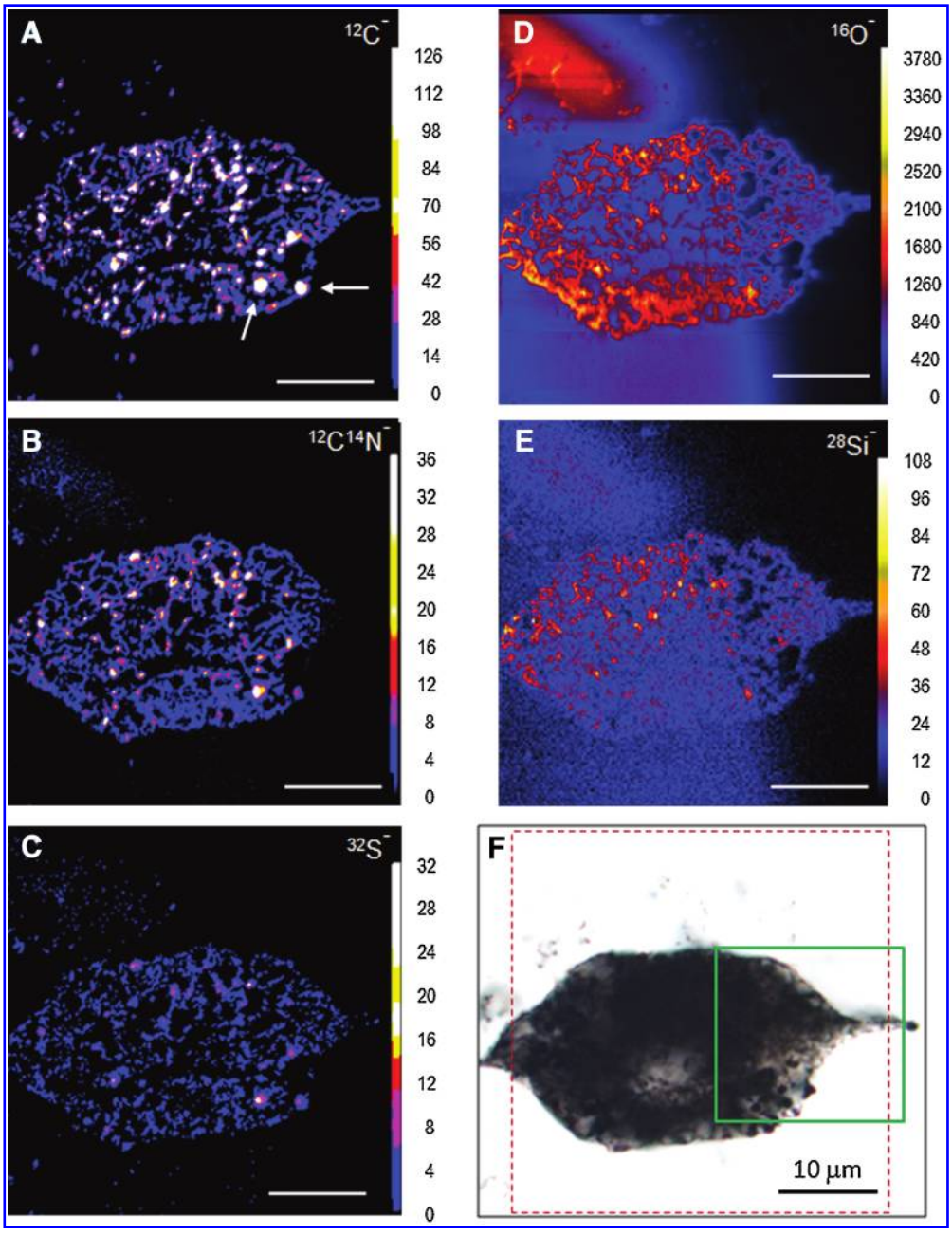

FIG. 4. NanoSIMS element maps of a "filled" spindle in chert from the Farrel Quartzite. (**A**–**E**) NanoSIMS maps for carbon ($^{12}C^-$), nitrogen ($^{12}C^{14}N^-$), sulfur ($^{32}S^-$), oxygen ($^{16}O^-$), and silicon ($^{28}Si^-$). Arrows in (A) point to examples of granules with high concentrations of $^{12}C^-$, $^{12}C^{14}N^-$, and $^{32}S^-$. Color bars and scales indicate yield of ions (intensity of response). The scales are set by the image processing software. (**F**) Optical photomicrograph in transmitted light of the spindle imaged by NanoSIMS in (A–E). Dashed red rectangle outlines area imaged by NanoSIMS in (A–E). Green rectangle outlines area imaged in Fig. 5. All scale bars are 10 μm.

Si^- and O^- in association with the microstructures are noticeably higher than responses from the surrounding chert matrix (Fig. 1D–E).

3.2. Large spheroids

Large spheroids in the Farrel Quartzite assemblage have diameters >10 μm and commonly between 20 and 60 μm (Sugitani *et al.*, 2007, 2009a, 2009b). These spheroids typically occur singly and appear to be preserved as folded or collapsed bodies, which suggests a somewhat delicate nature. Nearly 200 structures were measured by Sugitani *et al.* (2007). About half of those were completely hollow, and the other half were semi-hollow, with some internal bodies, reminiscent of the small spheroids.

The specimen imaged in NanoSIMS is shown in Fig. 2F. It is 30–35 μm in diameter, extensively folded, and apparently broken, with wisps of carbonaceous material hanging from an edge at the lower right of the specimen. The NanoSIMS element maps (Fig. 2A–E) illustrate the character of the

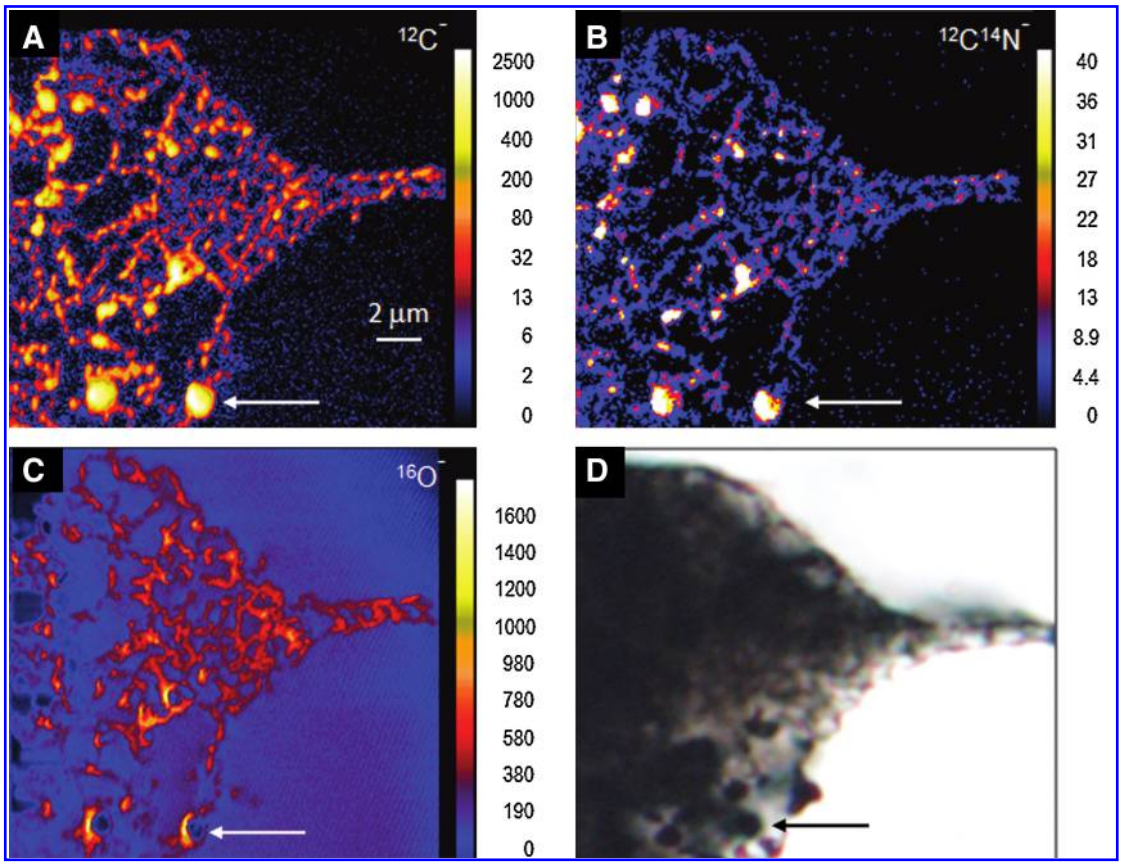

FIG. 5. High-resolution NanoSIMS element maps of the spindle of Fig. 4. (**A**–**C**) NanoSIMS maps for $^{12}C^-$, $^{12}C^{14}N^-$, and $^{16}O^-$. (**D**) Optical photomicrograph in transmitted light of the portion of the spindle imaged by NanoSIMS in (A–C) and shown by the green rectangle in Fig. 4. Arrows point to one of the granules with high $^{12}C^-$, $^{12}C^{14}N^-$, and $^{32}S^-$ (not shown) concentrations. (C) Illustrates oxygen concentrated around the perimeter of the granule (arrow). Color bars and scales indicate yield of ions (intensity of response). The scales are set by the image processing software. Scale bar in (A) applies to (A–D).

material that comprises this spheroid and show relationships among C^-, CN^-, and S^- that are identical to those for the small spheroids and suggestive of biogenicity. In addition, the C^-, CN^-, and S^- element concentrations of the large spheroid show the globular, aligned, and partially contiguous character that is reminiscent of remnants of cell walls (Oehler *et al.*, 2006). A comparison of element maps for O^- and Si^- with those for C^- and CN^- (Fig. 2A–B, 2C–D) shows a close correspondence between the organic material and the O^- and Si^-.

One difference between the NanoSIMS results for the large and small spheroids is that the bounding material of the large spheroids is more uniform in width than that of the small spheroids ($\sim$0.4 to 0.6 μm vs. 0.2 to 0.5 μm for the small spheroids). Another difference is the occurrence of numerous, subcircular granules with unusually high C^-, CN^-, and S^- content in the large spheroid. These granules occur within the remnants of the walls and have C^-, CN^-, and S^- responses 2–5 times higher in intensity than the majority of the wall-like material; the granules range from less than 0.3 μm to nearly 1 μm in diameter and are ringed by high responses for O^- and Si^- (arrows in Fig. 2A–E).

3.3. Spindles

The spindles are large, lenticular bodies, 20 to 40 μm in length and $\sim$15 to 35 μm in width (Sugitani *et al.*, 2007, 2009a, 2009b). They have tapered, spearlike appendages, 2–10 μm in length, at each end that, in individual specimens, seem to be connected to a flange that nearly encircles the spindle along the long axis. The spindles typically occur singly, in small groups, and in chains. Some are completely hollow, while others can be semi-hollow, including one or a few large cavities. Some appear to be completely filled by a network of carbonaceous material. While a few are folded, which suggests flexibility, most appear to be relatively robust and uncollapsed. These forms are abundant in the Farrel Quartzite, with hundreds of specimens having been documented (Sugitani *et al.*, 2007, 2009a, 2009b).

NanoSIMS element distributions of C^-, CN^-, S^-, O^-, and Si^- (Figs. 3–5) exhibit the same relationships to each other and to kerogen imaged in optical microscopy as occur in the small and large spheroids. The globular, aligned, and nearly contiguous character of the element concentrations are suggestive of wall-like remnants, with thicknesses ranging from 0.4 to 0.8 μm. In addition, the element maps show that the spindles, when they appear to be "filled," contain an intricate, reticulate network of organic material, all of which has similar thickness and element composition to the material that comprises the exterior of the spindle (Figs. 4–5). Figure 5 illustrates high-resolution NanoSIMS maps of C^-, CN^-, and O^- distributions in one of the spear-like appendages as well as in its connection to the body of the spindle. In these

images, the appendages and the body appear to be made of the same material. They both exhibit nearly identical element compositions and thicknesses, both consist of the carbonaceous reticulate network, and the connection between the appendage and the body is continuous with no evidence of any jointing or separation.

Like the large spheroids, the spindles contain numerous, subcircular granules with high C^-, CN^-, and S^- content (Figs. 3–5). The C^-, CN^-, and S^- responses of these granules are much higher than typical responses for the wall-like material (with intensities ranging from 2 to 10 times that of the majority of the wall-like material). Their size range is similar to that of the granules described from the large spheroids (less than 0.3 μm to nearly 1 μm in diameter), and they appear to be ringed by O^- and Si^- (especially well illustrated by arrows in Fig. 5).

The spindles in Fig. 3 show patches of material with atypically high CN^- response (arrow, Fig. 3B). The sulfur map shows similar regions of enrichment (arrow, Fig. 3C), but the carbon map appears to lack equivalent enrichment in those regions (Fig. 3A). The patches are somewhat angular in shape and adjacent to the cavities in the upper spindle of Fig. 3.

4. Discussion

4.1. Biogenicity

The correspondence and parallel variations among C^-, CN^-, and S^- in the Farrel Quartzite forms, coupled with the aligned (wall-like) and globular character of the element concentrations, suggest that the material comprising each of the structures analyzed is biogenic. Similar relationships have been seen in microfossils from the Bitter Springs Formation (Oehler *et al.,* 2006, 2008a, 2008b, 2008c, 2009) and in NanoSIMS analyses of modern cyanobacteria (Eybe *et al.,* 2007). In the modern cyanobacteria, it has been established that the NanoSIMS C^- and CN^- responses reflect the general morphology of the cells, and the S^- response reflects mainly protein distributions. Biogenicity of the spindles is discussed further in Section 4.6.

4.2. Syngeneity

The silicon and oxygen maps for each of the microstructures studied from the Farrel Quartzite show enhancements in these elements that are intimately associated with (and almost mimic) the carbon, nitrogen, and sulfur distributions.

A similar enhancement of silicon and oxygen was observed in the Bitter Springs microfossils (Oehler *et al.,* 2006), and it has been suggested that such enhancement of Si^- and O^- reflects the intimate association between silica and organic matter that results from silica permineralization (Oehler *et al.,* 2009). Silica permineralization involves nucleation of silica on organic surfaces, with initial weak bonding between the silica and functional groups in biological materials. Silica permineralization of biological structures is well known from (1) laboratory experiments (Oehler and Schopf, 1971; Oehler, 1976; Toporski *et al.,* 2002), (2) observations of natural silica nucleation on modern microbes (Phoenix *et al.,* 2000; Benning *et al.,* 2002; Renaut *et al.,* 2002), and (3) electron microscopic analyses of ancient microfossils (Moreau and Sharp, 2004). The latter study showed this intimate relationship in spheroidal microfossils from the ~2 Ga Gunflint Formation, where the wall was comprised of kerogen intimately intermixed with silica. The silica in the walls is very fine grained (100 by 300 nm) compared to the larger crystals (750 by 1000 nm) in the chert matrix, and similar size relationships have been observed in other studies of organic matter and silica (Oehler and Logan, 1977; Altermann and Schopf, 1995; Kempe *et al.,* 2005).

Such intimate intermixing of fine-grained silica and kerogen seems likely to account for the enhanced Si^- and O^- response in the walls of the Bitter Springs microfossils. The mechanism by which this occurs could be due to a "matrix effect" in NanoSIMS where Si^- and O^- from the silica associated with kerogen ionize more readily than Si^- and O^- from the matrix chert. Such preferential ionization could result from the comparatively small size of silica grains associated with the kerogen or the weak bonding at the kerogen-silica interface, or both. Alternatively, as carbonaceous material is known to sputter faster than chert (Dr. C. House, personal communication, 2008), the enhancement may result from the more rapid sputtering of the organic material during analysis, which would allow comparatively more silica mixed with the kerogen of the cell wall to be exposed to the primary ion beam. In either case, enhanced responses of Si^- and O^- associated with C^- and CN^- would be an indicator of an intimate association between silica and kerogen, and that is suggestive of the process of silica permineralization of biological materials. Since permineralization involves functional groups, it must occur prior to their loss through diagenesis, in the earliest stages of preservation. The fact that primary cherts preserve organic microfossils three-dimensionally, prior to their having been significantly compressed by burial, similarly attests to very early diagenetic occurrence of this process.

In contrast, carbonaceous matter in a secondary vein of the Eo-Archean Strelley Pool Chert shows no enhancement of Si^- associated with C^- or CN^- (Oehler *et al.,* 2009), which perhaps reflects a lack of intermixed, fine-grained silica such as has been imaged in the Gunflint microfossils (Moreau and Sharp, 2004). Petrographic relationships demonstrate that the vein formed after the chert matrix (Oehler *et al.,* 2009), and it and the carbonaceous material within are clearly epigenetic. The lack of intimately intermixed silica and carbon might reflect the fact that silica crystallization in the vein occurred later in diagenesis, when few functional groups remained in the carbonaceous material and the potential for bonding between silica and organic materials, therefore, was eliminated.

Thus, the spatial relationships among Si^-, O^-, C^-, and CN^- in the Farrel Quartzite microstructures provide support for their syngeneity with the chert matrix in which they occur. This conclusion is in line with (1) petrographic observations that the Farrel Quartzite microstructures are an integral part of the primary sedimentary fabric of the matrix chert (Sugitani *et al.,* 2007), and (2) results of laser-raman spectroscopy (Dr. J.W. Schopf, personal communication, 2009).

4.3. O^- response

In all specimens analyzed, the oxygen response is more intense than that of the silicon. This was true of the Bitter

Springs microfossils as well. The intensity of oxygen may result from a high ionization yield for oxygen in the cesium beam of the NanoSIMS, or it may, in part, reflect additional oxygen that was originally a constituent of sugars, proteins, or lipids, as has been shown by the NanoSIMS mapping of modern cyanobacteria (Eybe *et al.,* 2007).

4.4. Granules with high yields of C^-, CN^-, and S^-

The granules have only been seen in the large spheroids and spindles; they do not appear in the small spheroids analyzed to date. In the granules, the C^-, CN^-, and S^- yields appear to vary in parallel. In the high-resolution C^- and CN^- maps (Fig. 5A–B), the correspondence of high C^- and CN^- is apparent. Figure 4A–C also illustrates the correspondence of high S^- with high C^- and high CN^-. This correspondence suggests that the granules may have been derived from organic constituents similar to those that make up the bulk of the large spheroids and spindles. The fact that the granules are associated with enhanced silicon and oxygen concentrations at their perimeters (Figs. 4D–E, 5C) suggests that the granules were present prior to silicification. In all characteristics mentioned above, the granules are different from the secondary carbonaceous material that was analyzed by NanoSIMS from the secondary vein in a sample of the Strelley Pool Chert (Oehler *et al.,* 2009). That material, which seems likely to have been mobilized by hydrothermal activity, is comprised of dispersed, angular particles that are very low in CN^-, show no parallelism between intensities of C^- and CN^-, and show no equivalent enhancements in Si^- beyond the concentrations measured in the chert matrix.

4.5. Patches with high yields of CN^- and S^-

The patches with high CN^- and S^- yields are atypical of the organic structures in the Farrel Quartzite. They occur only in association with a partially hollow spindle (Fig. 3). These patches differ from the granules described above in lacking correspondingly high C^- responses and in their more irregular, angular shapes and larger size range ($\sim$0.1 to 1.5 μm). Because the e-gun was always used, these patches are unlikely to be an effect of charging. Since all the Farrel Quartzite samples were analyzed under the same conditions and since the concentrations of both CN^- and S^- are much higher than encountered in other specimens, it is doubtful that the high CN^- and S^- patches are artifacts of instrumental effects.

Nevertheless, it is not clear whether the nitrogen and sulfur in these patches are original attributes or whether they might involve diagenetic addition to an existing carbonaceous "skeleton." If nitrogen and sulfur were added diagenetically, this must have occurred during the earliest phases of preservation, as Si^- and O^- surround the patches, which implies that the CN^-- and S^--enriched patches were present during the process of silica permineralization (Oehler *et al.,* 2009).

The enriched patches are adjacent to cavities in the partially hollow spindle of Fig. 3. The cavities have rounded edges and, in this regard, resemble gas vacuoles that occur in prokaryotic and some eukaryotic cells. In modern organisms, gas vacuoles commonly contain nitrogen- and sulfur-bearing compounds that serve purposes ranging from buoyancy control to storage of nutrients or waste products (Walsby, 1972; Spencer and King, 1989; Sayama, 2001). Thus, one possibility is that degraded gas vacuoles in the spindles might have been a source for added nitrogen and sulfur in the patches. However, only one specimen of a partially hollow spindle was imaged in NanoSIMS, and such relationships are speculative. Future work, aimed at obtaining NanoSIMS element maps of more examples of partially hollow spindles, should help in assessment of the significance of these patches.

4.6. Spindles

The spindles (Figs. 3–5) are the most enigmatic forms in this assemblage. Some examples have a nearly geometric shape, and this has led to concern that they could be pseudofossils, formed by aggregation of particulate organic matter on crystal surfaces (similar to processes described by García-Ruiz *et al.,* 2002, 2003). While there is no evidence of such crystals today (the spindles are permineralized by cryptocrystalline chert), there is the possibility that large lenticular crystals were present initially but were lost during early diagenesis. Sugitani *et al.* (2007, 2009a) assessed potential abiotic origins for the spindles and concluded that the various abiotic scenarios are unlikely and the spindles are highly probable microfossils. Recent work by Grey and Sugitani (2009) supports this interpretation. These authors showed that several spindles could be isolated from acid maceration, which indicates a coherence of structure that would be unlikely in aggregates of particulate material. The results from NanoSIMS further attest to a biogenic origin by demonstrating the globular, aligned, and semi-contiguous C^-, CN^-, and S^- concentrations that make up the material of the spindles; the parallelism among their C^-, CN^-, and S^- responses; and their reticulate internal networks (which would be difficult to reconcile with any process of surface aggregation).

While the large size and structural complexity of the spindles seem surprising for Archean-aged organisms, similar forms have been identified in two even older Eo-Archean deposits (3.44–3.26 Ga sediments of the Onverwacht Group of South Africa; Walsh, 1992). Nevertheless, the biological affinities of the spindles are uncertain. Their apparent robustness might support a derivation from a resistant precursor that was adapted for survival on an early Earth subjected to extreme heat, UV, or desiccating conditions. Walsh (1992) noted the possibility that the spindles in the Onverwacht Group might have analogues in resistant bacterial spores or cysts that could have afforded a survival advantage on a young Earth where periodic impacts may have generated nearly planet-sterilizing heat.

Sugitani *et al.* (2009a, 2009b) suggested that there may be an association between some of the smaller spheroids in the Farrel Quartzite deposit and the spindles, where the spindles might represent a resistant outer wall of the resting stage of an organism and the small spheroids could represent endospores of that same organism. In fact, in a few images, the spindles appear to contain small spore-like spheroids, and perhaps the reticulate internal network that has been imaged by NanoSIMS might be related to such spores. Alternatively, the reticulate network may represent an architecture developed during an early evolutionary phase of morphological

experimentation that may have no analogy among modern microbial forms.

The Archean age of the spindles might suggest prokaryotic affinities. Although their large sizes are more typical of eukaryotic microbes (Schopf, 1992), some prokaryotic spores can reach large and even macroscopic sizes (Walsh, 1992). Certainly the organizational complexity of the spindles (with their flanges, spearlike appendages, and internal reticulate networks) attests to a relatively advanced morphology.

Recent biomarker studies by Waldbauer *et al.* (2009) concluded that biochemical innovation in the Archean laid the groundwork for all three domains of life (Bacteria, Archaea, and Eukaryota); accordingly, it is even conceivable that the spindles could be early representatives of the Domain Eukaryota. At a minimum, results from our work support the existence of a diverse microbiota by 3 Ga with individual constituents (the spindles) exhibiting an advanced level of structural organization. These results align with conclusions from Waldbauer *et al.* (2009). Both studies point to surprising evolutionary diversification in the Archean.

5. Conclusions

NanoSIMS element distributions for small spheroids, large spheroids, and spindles preserved in chert of the ~3 Ga Farrel Quartzite suggest that each of these is a bona fide microfossil of an Archean microorganism. This assemblage, then, joins the few handfuls of examples of organically preserved microbiotas of Archean age (summarized in Schopf, 2006). And these microbiota join a host of recent stromatolitic and geochemical results indicative of a multifaceted Archean biosphere (references listed in the Introduction). Together, these lines of evidence are building a picture of Archean life that was surprisingly diverse and probably metabolically and ecologically more advanced than might have been surmised just a few years ago.

The spindle-like forms are of particular interest because of their large size and morphological complexity—with flanges, spearlike appendages, and an intricate internal network that is integral to both the body and appendages. This level of organization is in contrast to that of the simpler and generally smaller spheroids and filaments common to many Precambrian microbiotas. The spindles are abundant in the Farrel Quartzite cherts, and they exhibit an apparent robustness that might suggest an origin from a resistant organism—possibly one that developed on an environmentally hostile young planet.

Thus, the microbiota of the Farrel Quartzite is notable, not only because it comprises a ~3 Ga assemblage of organically preserved microfossils but also because it is diverse and includes spindle-shaped forms with relatively advanced morphology. If the recent suggestion by Waldbauer *et al.* (2009) is correct—that biochemical innovation in the Archean laid the groundwork for development of the three domains of life—then our work, which supports the biogenicity and syngeneity of the Farrel Quartzite forms, complements and aligns with this view of early evolution on Earth.

Evolution of life on other planets, similarly, may involve a phase of early innovation. This may augur well for the possibility that primitive, extraterrestrial life could adapt to changing or adverse conditions by ready development of diversity in form and biochemistry and, accordingly, that such extraterrestrial life may have been relatively long-lived.

NanoSIMS is a relatively new technology that has allowed us to look at submicron-scale elemental composition of organic material in ancient sediments. We are gaining an understanding of characteristics that typify fragments of ancient cells on Earth. This capability can provide insights into the origin of remnants of organic matter that may be found in extraterrestrial materials and gives us a new tool with which to assess the significance of poorly preserved materials we are likely to encounter in earliest Archean samples from Earth and in meteorites or other extraterrestrial samples.

Acknowledgments

We are grateful for the support of the Astromaterials Research and Exploration Science Directorate at NASA Johnson Space Center; the Australian Centre for Astrobiology; the Department of Environmental Engineering and Architecture in the Graduate School of Environmental Studies, Nagoya University; and the Centre National de la Recherche Scientifique (CNRS). Doctor L. Remusat (Laboratoire d'Etude de la Matière Extraterrestre, CNRS) assisted with image-processing software. This work was additionally supported by a PNP grant from the CNRS to F.R. and a NASA Exobiology and Evolutionary Biology Grant to E.K.G. and D.O. Financial support to K.S. from the Japan Society for the Promotion of Science (the Joint Research Program, Japan-Australia and a grant-in-aid, No. 19340150) is gratefully acknowledged. The National NanoSIMS facility at the Muséum National d'Histoire Naturelle was established by funds from the CNRS, Région Île de France, Ministère délégué à l'Enseignement supérieur et à la Recherche, and the Muséum itself.

Abbreviations

e-gun, electron gun; NanoSIMS, nano-scale secondary ion mass spectrometry.

References

Allwood, A.C., Walter, M.R., Kamber, B.S., Marshall, C.P. and Burch, I.W. (2006) Stromatolite reef from the Early Archaean era of Australia. *Nature* 441:714–718.

Allwood, A.C., Grotzinger, J.P., Knoll, A.H., Burch, I.W., Anderson, M.S., Coleman, M.L., and Kanik, I. (2009) Controls on development and diversity of Early Archean stromatolites. *Proc. Natl. Acad. Sci. U.S.A.* 106:9548–9555.

Altermann, W. and Kazmierczak, J. (2003) Archean microfossils: a reappraisal of early life on Earth. *Res. Microbiol.* 154: 611–617.

Altermann, W. and Schopf, J.W. (1995) Microfossils from the Neoarchean Campbell Group, Griqualand West Sequence of the Transvaal Supergroup, and their paleoenvironmental and evolutionary implications. *Precambrian Res.* 75:65–90.

Beaumont, V. and Robert, F. (1999) Nitrogen isotope ratios of kerogens in Precambrian cherts: a record of the evolution of atmosphere chemistry? *Precambrian Res.* 96:63–82.

Benning, L.G., Phoenix, V., Yee, N., Tobin, J.J., Konhauser, K.O., and Mountain, B.W. (2002) Molecular characterization of cyanobacterial cells during silicification: a synchrotron-based infrared study. *Geochemistry of the Earth's Surface* 6:259–263.

Brasier, M., McLoughlin, M., Green, O., and Wacey, D. (2006) A fresh look at the fossil evidence for early Archaean cellular life. *Philos. Trans. R. Soc. Lond., B, Biol. Sci.* 361:887–902.

Brocks, J.J., Logan, G.A., Buick, R., and Summons, R.E. (1999) Archean molecular fossils and the early rise of eukaryotes. *Science* 285:1033–1036.

De Gregorio, B.T. and Sharp, T.G. (2007) *In situ* correlated electron and X-ray microscopy of putative Archean biosignatures: a novel approach for assessing the biogenicity of ancient organic matter [Paper No. 166-3]. In *Abstracts with Programs*, Vol. 39, Geological Society of America, Boulder, CO, p 448.

De Gregorio, B.T., Sharp, T.G., Flynn, G.J., Wirick, S., and Hervig, R.L. (2009) Biogenic origin for Earth's oldest putative microfossils. *Geology* 37:631–634.

Derenne, S., Robert, F., Skrzypczak-Bonduelle, A., Gourier, D., Binet, L., and Rouzaud, J.-N. (2008) Molecular evidence for life in the 3.5 billion year old Warrawoona Chert. *Earth Planet. Sci. Lett.* 272:476–480.

Duck, L.J., Glikson, M., Golding, S.D., and Webb, R.E. (2007) Microbial remains and other carbonaceous forms from the 3.24 Ga Sulfur Springs black smoker deposit, Western Australia. *Precambrian Res.* 154:205–220.

Eigenbrode, J.L. and Freeman, K.H. (2006) Late Archean rise of aerobic microbial ecosystems. *Proc. Natl. Acad. Sci. U.S.A.* 103: 15759–15764.

Eybe, T., Audinot, J.-N., Migeon, H.-N., Bohn, T., and Hoffmann, L. (2007) Mapping the elemental composition of cyanobacteria with the NanoSIMS 50. *Microsc. Microanal.* 13(Supplement 3): 178–179.

García-Ruiz, J.M., Carnerup, A.M., Christy, A.G., Welham, N.J., and Hyde, S.T. (2002) Morphology: an ambiguous indicator for biogenicity. *Astrobiology* 2:335–351.

García-Ruiz, J.M., Hyde, S.T., Carnerup, A.M., Christy, A.G., Van Kranendonk, M.J., and Welham, N.J. (2003) Self-assembled silica-carbonate structures and detection of ancient microfossils. *Science* 302:1194–1197.

Grey, K. and Sugitani, K. (2009) Palynology of Archean microfossils (c. 3.0 Ga) from the Mount Grant area, Pilbara Craton, Western Australia: further evidence of biogenicity. *Precambrian Res.* 173:60–69.

Hofmann, H.J., Grey, K., Hickman, A.H., and Thorpe, R.I. (1999) Origin of 3.45 Ga coniform stromatolites in Warrawoona Group, Western Australia. *Geol. Soc. Am. Bull.* 111: 1256–1262.

Javaux, E.J., Marshall, C.P., and Bekker, A. (2010) Organic-walled microfossils in 3.2-billion-year-old shallow-marine siliciclastic deposits. *Nature* 463:934–938.

Kempe, A., Wirth, R., Altermann, W., Stark, R.W., Schopf, J.W., and Heckl, W.M. (2005) Focused ion beam preparation and *in situ* nanoscopic study of Precambrian acritarchs. *Precambrian Res.* 140:36–54.

Lindsay, J.F., Brasier, M.D., McLoughlin, N., Green, O.R., Fogel, M., McNamara, K.M., Steele, A., and Mertzman, S.A. (2003) Abiotic Earth—establishing a baseline for earliest life, data from the Archean of Western Australia [abstract 1137]. In *34th Lunar and Planetary Science Conference,* Lunar and Planetary Institute, Houston.

Marshall, C.P., Love, G.D., Snape, C.E., Hill, A.C., Allwood, A.C., Walter, M.R., Van Kranendonk, M.J., Bowden, S.A., Sylvia, S.P., and Summons, R.E. (2007) Structural characterization of kerogen in 3.4 Ga Archaean cherts from the Pilbara Craton, Western Australia. *Precambrian Res.* 155:1–23.

Moorbath. S. (2005) Dating earliest life. *Nature* 434:155.

Moreau, J.W. and Sharp, T.M. (2004) A transmission electron microscopy study of silica and kerogen biosignatures in 1.9 Ga Gunflint microfossils. *Astrobiology* 4:196–210.

Oehler, D.Z., Robert, F., Mostefaoui, S., Meibom, A., Selo, M., and McKay, D.S. (2006) Chemical mapping of Proterozoic organic matter at sub-micron spatial resolution. *Astrobiology* 6:838–850.

Oehler, D.Z., Robert, F., Meibom, A., Mostefaoui, S., Selo, M., Walter, M.R., Sugitani, K., Allwood, A., Mimura, K., and Gibson, E.K. (2008a) "Nano" scale biosignatures and the search for extraterrestrial life [abstract 1303]. In *39th Lunar and Planetary Science Conference,* Lunar and Planetary Institute, Houston.

Oehler, D.Z., Robert, F., Meibom, A., Mostefaoui, S., Selo, M., Walter, M.R., Sugitani, K., Allwood, A., and Gibson, E.K. (2008b) NanoSIMS sheds light on the origin and significance of Early Archean organic microstructures from the Pilbara of Australia. *Astrobiology* 8:324.

Oehler, D.Z., Robert, F., Chaussidon, M., and Gibson, E.K. (2008c) Bona fide biosignatures: insights from combined NanoSIMS-SIMS. In *18th Annual V.M. Goldschmidt Conference,* The Geochemical Society, Saint Louis, MO, p A698.

Oehler, D.Z., Robert, F., Walter, M.R., Sugitani, K., Allwood, A., Meibom, A., Mostefaoui, S., Selo, M.R., Thomen, A., and Gibson, E.K. (2009) NANOSIMS: insights to biogenicity and syngeneity of Archaean carbonaceous structures. *Precambrian Res.* 173:70–78.

Oehler, J.H. (1976) Experimental studies in Precambrian paleontology: structural and chemical changes in blue-green algae during simulated fossilization in synthetic chert. *Geol. Soc. Am. Bull.* 87:117–129.

Oehler, J.H. and Logan, R.G. (1977) Microfossils, cherts, and associated mineralization in the Proterozoic McArthur (H.Y.C.) lead-zinc-silver deposit. *Econ. Geol.* 72:1393–1409.

Oehler, J.H. and Schopf, J.W. (1971) Artificial microfossils: experimental studies of permineralization of blue-green algae in silica. *Science* 174:1229–1231.

Phoenix, V.R., Adams, D.G., and Konhauser, K.O. (2000) Cyanobacterial viability during hydrothermal biomineralization. *Chem. Geol.* 169:329–338.

Rasmussen, B. (2000) Filamentous microfossils in a 3235-milliion-year-old volcanogenic massive sulphide deposit. *Nature* 405: 676–679.

Rasmussen, B., Fletcher, I.R., Brocks, J.J., and Kilburn, M.R. (2008) Reassessing the first appearance of eukaryotes and cyanobacteria. *Nature* 455:1101–1104.

Rasmussen, B., Blake, T.S., Fletcher, I.R., and Kilburn, M.R. (2009) Evidence for microbial life in synsedimentary cavities from 2.75 Ga terrestrial environments. *Geology* 37:423–426.

Renaut, R.W., Jones, B., Tiercelin, J.–J., and Tarits, C. (2002) Sublacustrine precipitation of hydrothermal silica in rift lakes: evidence from Lake Baringo, central Kenya Rift Valley. *Sediment. Geol.* 148:235–257.

Sayama, M. (2001) Presence of nitrate-accumulating sulfur bacteria and their influence on nitrogen cycling in a shallow coastal marine sediment. *Appl. Environ. Microbiol.* 67:3481–3487.

Schopf, J.W. (1968) Microflora of the Bitter Springs Formation, Late Precambrian, central Australia. *J. Paleontol.* 42:651–668.

Schopf, J.W. (1992) Proterozoic prokaryotes: affinities, geologic distribution, and evolutionary trends. In *The Proterozoic Biosphere,* edited by J.W. Schopf and C. Klein, Cambridge University Press, Cambridge, pp 195–218.

Schopf, J.W. (1993) Microfossils of the Early Archean Apex Chert: new evidence of the antiquity of life. *Science* 260:640–646.

Schopf, J.W. (2006) Fossil evidence of Archaean life. *Philos. Trans. R. Soc. Lond., B, Biol. Sci.* 361:869–885.

Schopf, J.W. and Blacic, J.M. (1971) New microorganisms from the Bitter Springs Formation (Late Precambrian) of the north-central Amadeus Basin, Australia. *J. Paleontol.* 45:925–961.

Schopf, J.W. and Walter, M.R. (2007) Earliest evidence of life on earth. *Precambrian Res.* 158:139–140.

Schopf, J.W., Kudryavtsev, A.B., Czaja, D., and Tripathi, A.B. (2007) Evidence of Archean life: stromatolites and microfossils. *Precambrian Res.* 158:141–155.

Spencer, C.N. and King, D.L. (1989) Role of light, carbon dioxide and nitrogen in regulation of buoyancy, growth and bloom formation of *Anabaena flos-aquae*. *J. Plankton Res.* 11:283–296.

Sugitani, K., Grey, K., Allwood, A., Nagaoka, T., Mimura, K., Minami, M., Marshall, C.P., Van Kranendonk, M.J., and Walter, M.R. (2007) Diverse microstructures from Archaean chert from the Mount Goldsworthy–Mount Grant area, Pilbara Craton, Western Australia: microfossils, dubiofossils, or pseudofossils? *Precambrian Res.* 158:228–262.

Sugitani, K., Grey, K., Nagaoka, T., and Mimura, K. (2009a) Three-dimensional morphological and textural complexity of Archean putative microfossils from the northeastern Pilbara Craton: indications of biogenicity of large (>15 μm) spheroidal and spindle-like structures. *Astrobiology* 9:603–615.

Sugitani, K., Grey, K., Nagaoka, T., Mimura, K., and Walter, M.R. (2009b) Taxonomy and biogenicity of Archaean spheroidal microfossils (*ca.* 3.0 Ga) from the Mount Goldsworthy–Mount Grant area in the northeastern Pilbara Craton, Western Australia. *Precambrian Res.* 173:50–59.

Toporski, J.K., Steele, A., Westall, F., Thomas-Keprta, K.L., and McKay, D.S. (2002) The simulated silicification of bacteria—new clues to the modes and timing of bacterial preservation and implications for the search for extraterrestrial microfossils. *Astrobiology* 2:1–26.

Waldbauer, J.R., Sherman, L.S., Sumner, D.Y., and Summons, R.E. (2009) Late Archean molecular fossils from the Transvaal Supergroup record the antiquity of microbial diversity and aerobiosis. *Precambrian Res.* 169:28–47.

Walsby, A.E. (1972) Structure and function of gas vacuoles. *Bacteriol. Rev.* 36:1–32.

Walsh, M.M. (1992) Microfossils and possible microfossils from the Early Archean Onverwacht Group, Barberton Mountain Land, South Africa. *Precambrian Res.* 54:271–293.

Walter, M.R., Buick, R., and Dunlop, J.S.R. (1980) Stromatolites 3400–3500 Myr old from the North Pole area, Western Australia. *Nature* 284:443–445.

Van Zuilen, M.A., Chaussidon, M., Rollion-Bard, C., and Marty, G. (2007) Carbonaceous cherts of the Barberton greenstone belt, South Africa: isotopic, chemical and structural characteristics of individual microstructures. *Geochim. Cosmochim. Acta* 71:655–669.

Address correspondence to:
Dorothy Z. Oehler
Astromaterials Research and Exploration Science
NASA, Johnson Space Center
2101 NASA Parkway
Houston, TX 77058
USA

E-mail: dorothy.z.oehler@nasa.gov

Submitted 11 September 2009
Accepted 6 March 2010

This article has been cited by:

1. Carrine E. Blank, S. Lin. 2013. Origin and early evolution of photosynthetic eukaryotes in freshwater environments: reinterpreting proterozoic paleobiology and biogeochemical processes in light of trait evolution. *Journal of Phycology* **49**:6, 1040-1055. [CrossRef]
2. Zhenbing She, Paul Strother, Gregory McMahon, Larry R. Nittler, Jianhua Wang, Jianhua Zhang, Longkang Sang, Changqian Ma, Dominic Papineau. 2013. Terminal Proterozoic cyanobacterial blooms and phosphogenesis documented by the Doushantuo granular phosphorites I: In situ micro-analysis of textures and composition. *Precambrian Research* **235**, 20-35. [CrossRef]
3. Kevin Lepot, Kenneth H. Williford, Takayuki Ushikubo, Kenichiro Sugitani, Koichi Mimura, Michael J. Spicuzza, John W. Valley. 2013. Texture-specific isotopic compositions in 3.4Gyr old organic matter support selective preservation in cell-like structures. *Geochimica et Cosmochimica Acta* **112**, 66-86. [CrossRef]
4. C. H. House, D. Z. Oehler, K. Sugitani, K. Mimura. 2013. Carbon isotopic analyses of ca. 3.0 Ga microstructures imply planktonic autotrophs inhabited Earth's early oceans. *Geology* **41**:6, 651-654. [CrossRef]
5. Kenichiro Sugitani, Koichi Mimura, Tsutomu Nagaoka, Kevin Lepot, Makoto Takeuchi. 2013. Microfossil assemblage from the 3400Ma Strelley Pool Formation in the Pilbara Craton, Western Australia: Results form a new locality. *Precambrian Research* **226**, 59-74. [CrossRef]
6. Michael Wiedenbeck, Roxana Bugoi, M. John M. Duke, Tibor Dunai, Jacinta Enzweiler, Mary Horan, Klaus Peter Jochum, Kathryn Linge, Jan Košler, Silke Merchel, Luiz F.G. Morales, Lutz Nasdala, Roland Stalder, Paul Sylvester, Ulrike Weis, Arnaud Zoubir. 2012. GGR Biennial Critical Review: Analytical Developments Since 2010. *Geostandards and Geoanalytical Research* **36**:4, 337-398. [CrossRef]
7. David Wacey, Sarath Menon, Leonard Green, Derek Gerstmann, Charlie Kong, Nicola Mcloughlin, Martin Saunders, Martin Brasier. 2012. Taphonomy of very ancient microfossils from the #3400Ma Strelley Pool Formation and #1900Ma Gunflint Formation: New insights using a focused ion beam. *Precambrian Research* **220-221**, 234-250. [CrossRef]
8. Martin D. Brasier, David Wacey. 2012. Fossils and astrobiology: new protocols for cell evolution in deep time. *International Journal of Astrobiology* **11**:04, 217-228. [CrossRef]
9. J. William Schopf, Jack D. Farmer, Ian S. Foster, Anatoliy B. Kudryavtsev, Victor A. Gallardo, Carola Espinoza. 2012. Gypsum-Permineralized Microfossils and Their Relevance to the Search for Life on Mars. *Astrobiology* **12**:7, 619-633. [Abstract] [Full Text HTML] [Full Text PDF] [Full Text PDF with Links]
10. D Wacey. 2012. Earliest evidence for life on Earth: an Australian perspective. *Australian Journal of Earth Sciences* **59**:2, 153-166. [CrossRef]
11. ARTHUR HUGH HICKMAN. 2012. Review of the Pilbara Craton and Fortescue Basin, Western Australia: Crustal evolution providing environments for early life. *Island Arc* **21**:1, 1-31. [CrossRef]
12. Mathias Senoner, Wolfgang E. S. Unger. 2012. SIMS imaging of the nanoworld: applications in science and technology. *Journal of Analytical Atomic Spectrometry* **27**:7, 1050. [CrossRef]
13. Can Su, Liping Lei, Yanqing Duan, Ke-Qin Zhang, Jinkui Yang. 2011. Culture-independent methods for studying environmental microorganisms: methods, application, and perspective. *Applied Microbiology and Biotechnology* . [CrossRef]
14. Volker Thiel, Peter Sjövall. 2011. Using Time-of-Flight Secondary Ion Mass Spectrometry to Study Biomarkers. *Annual Review of Earth and Planetary Sciences* **39**:1, 125-156. [CrossRef]
15. References 493-557. [CrossRef]
16. Kenichiro Sugitani, Kevin Lepot, Tsutomu Nagaoka, Koichi Mimura, Martin Van Kranendonk, Dorothy Z. Oehler, Malcolm R. Walter. 2010. Biogenicity of Morphologically Diverse Carbonaceous Microstructures from the ca. 3400 Ma Strelley Pool Formation, in the Pilbara Craton, Western Australia. *Astrobiology* **10**:9, 899-920. [Abstract] [Full Text HTML] [Full Text PDF] [Full Text PDF with Links]